

Phased Passive Fluxgate Control of Structural Changes in Low-Carbon and Low-Alloy Steels of Construction Machines



Alexander Scherbakov , Anna Babanina , Elena Kuzbagarova , and Artur Kuzbagarov 

Abstract The initial structure of metals and alloys determines their mechanical properties. They can differ significantly in various elements of welded metal structures, as well as in the zones and sections of welded joints. Plastic deformation can occur in hazardous areas of stress concentration of elements of operated metal structures. In this work, studies were carried out on samples of low-carbon steel 08 ps and low-alloy steel 10KhSND, which were subjected to thermal cycling in the following conditions: as delivered state; as delivered + annealing at 900 °C; as delivered + cold rolling for the degree of deformation $\varepsilon = 50\%$. The formation of a fine-grained structure during thermal cycling was monitored by a passive fluxgate method, as well as by microstructural analysis and hardness testing. The value of the stray magnetic field strength H_p was measured. As a result of the conducted studies, a relationship was established between the magnetic parameter H_p and structural changes in steels during thermal cycling.

Keywords Welded metal structures · Construction machines · Passive fluxgate control

1 Introduction

In the manufacture of welded metal structures of construction machines, low-carbon and low-alloy steels are widely used, which in the as delivered state (hot-rolled, cold-rolled, after various types of heat treatment) have a different initial microstructure

A. Scherbakov (✉) · E. Kuzbagarova · A. Kuzbagarov
Saint Petersburg State University of Architecture and Civil Engineering, Vtoraya
Krasnoarmeiskaya Street, 4, Saint Petersburg, Russia 190005

A. Babanina
Peter the Great St. Petersburg Polytechnic University, Polytechnicheskaya Street, 29, Saint
Petersburg, Russia 195251

(coarse-grained, fine-grained, plastically deformed). In addition, structural heterogeneity is inherent in welded joints: a cast structure in the welded seam, coarse-grained in the overheating area, and fine-grained in the area of complete recrystallization. Considering that the initial structure determines the mechanical properties of metals and alloys, they can significantly differ in various elements of welded metal structures, as well as in the zones and sections of welded joints. Besides, plastic deformation can occur in hazardous areas of stress concentration of elements of operated metal structures. In this regard, it is advisable to conduct study to assess the degree of influence of the metal structure on the operational reliability of elements of metal structures of construction machines.

Numerous experimental studies carried out show that the strength of annealed metals and alloys tested at sufficiently low temperatures, when the recovery processes are difficult, increases with grain refinement. Thus, with a decrease in the grain size in the range from 10 to 1 μm , the yield stress, flow stress at various values of deformation, ultimate strength, hardness and fatigue strength of a significant number of metals and alloys increase.

The fine grain structure has a significant effect on structural strength. Iron and other metals with a body-centered lattice tend to transition from a ductile to a brittle state at a certain tensile test temperature and low strain rates. At temperatures below the brittleness threshold, the sample collapses without necking at low plasticity values. The impact toughness of steel Jn-744 greatly depends on the grain size. When it changes from 2 to 25 μm , the transition temperature from ductile to brittle fracture shifts towards higher temperatures from -130 to -45 $^{\circ}\text{C}$. The observed difference in the properties of steel is caused solely by the difference in the dispersion of the structure, since the chemical composition of the phases of both fine-grained and coarse-grained material was the same.

Since with a decrease in the grain size at low temperatures, the yield stress, strength, hardness, fatigue strength, and impact toughness increase, obtaining a fine-grained structure is of independent importance for increasing the strength properties of metals. This phenomenon can be used when strengthening the elements of metal structures of construction machines in hazardous stress concentration zones due to the refinement of the metal structure according to the modes of thermal cycling developed in the dissertation work.

One of the conditions for ensuring a given level of quality of metal structures is the correct use of existing and development of new devices and methods of non-destructive testing. At the same time, in order to reduce production costs and reduce the cost of products, it is desirable to carry out non-destructive testing not only after final processing, but also at individual stages of their manufacture. Such possibilities are provided by the passive fluxgate control method, which was used for magnetic control of structural transformations in steels during thermal cycling.

Thermal cycling is one of the most effective ways to obtain a microstructure with a given degree of dispersion. It is based on the constant accumulation, from cycle to cycle of heating and cooling, positive changes in the structure of metals. At the same time, an important feature of the metal heating-cooling cycle is its intensity, and what is the most important is the absence or presence of short exposures at

extreme temperatures, as well as the optimal range of temperature variation. During thermal cycling, additional sources of influence on the structure appear, characteristic only of the process of continuous temperature change, the main of which are phase transformations, temperature gradients, thermal (volumetric) and interfacial stresses caused by the difference in thermophysical characteristics of the phases constituting the structure [1–5].

The use of thermal cycling to obtain structures with a given degree of dispersion is important for two reasons. First, it becomes possible to obtain metal microstructures characteristic of the factory-supplied rolled metal used in the manufacture of welded metal structures and structural heterogeneity of welded joints. Secondly, to obtain a fine-grained structure, which is unattainable with conventional types of heat treatment [6–9]. This, in turn, makes it possible to use the method of thermal cycling to restore the metal structure and enhance hazardous stress concentration zones in the elements of welded metal structures and welded joints with structural heterogeneity, due to the formation of a finer-grained structure with increased strength properties in them. It should be noted that the development of thermal cycling modes in each specific case has an individual character and cannot be mechanically transferred from one material to another.

2 Materials and Methods

For research, samples were cut out of 08 ps mild steel and 10KhSND low-alloy steel, which were subjected to thermal cycling in the following conditions: as delivered condition; as delivered + annealing at 900 °C; as delivered + cold rolling for the degree of deformation $\varepsilon = 50\%$.

The formation of a fine-grained structure in the course of thermal cycling was controlled by the passive fluxgate method, as well as by microstructural analysis and hardness testing. The measurement of the stray magnetic field strength H_p was carried out by a two-channel fluxgate transducer installed perpendicular to the sample surface. On each sample, in its middle part along the axial line, the H_p values were recorded in three control zones spaced 30 mm apart from each other. The H_p values were measured both before the first thermal cycle and at the end of each heating–cooling cycle. To plot the dependences of the H_p values on the number of cycles, the averaged H_p value of the indicated control zones was taken. The number of cycles was chosen as follows: 1, 2, 3, 4, 5, 7, and 10.

3 Results and Discussion

Figure 1 shows the dependence of H_p on the number of cycles during thermal cycling of steels 08 ps and 10KhSND in different initial states.

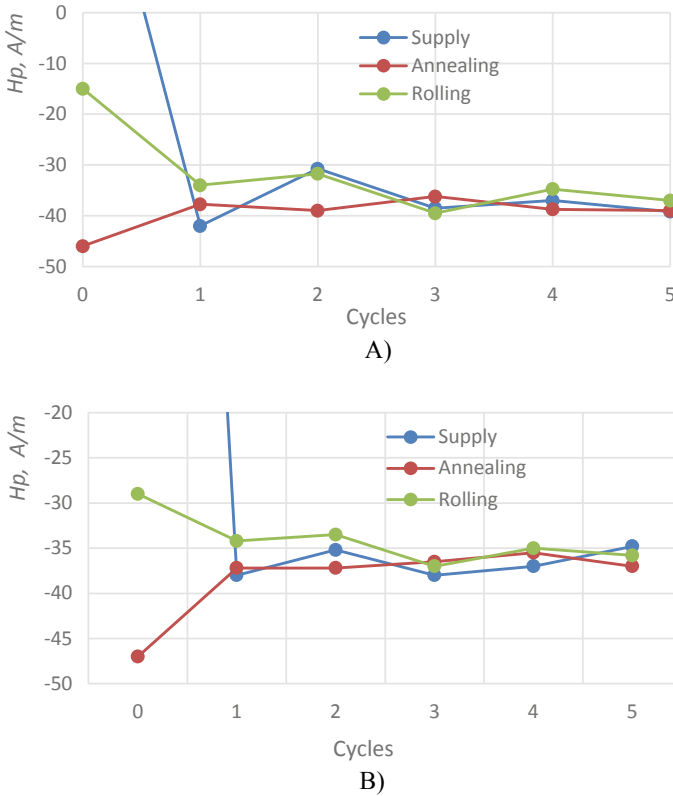


Fig. 1 Dependence of the magnetic field strength H_p on the number of cycles during thermal cycling of steels 08 ps (a) and 10KhSND (b) in different initial structural states

We can see that the greatest changes in the values of H_p for all studied steels are observed during the first two or three thermal cycles. In this case, the magnetic prehistory of the samples is erased, as evidenced by the change from the positive sign to negative and the convergence of the H_p values. With an increase in the number of cycles, the magnetic field strength values stabilize, which is noticeable from a decrease in the spread in H_p values. An increase in the number of cycles from 5 to 7 and 10 has almost no effect on the change in the magnetic parameter H_p .

During the thermal cycling of the samples in the as delivered state, there is a sharp change in the value of the stray magnetic field strength after the first cycle (Fig. 2). During subsequent thermal cycles, negative values of H_p do not change their sign.

Annealing before thermal cycling shifts the initial values of H_p to the region of negative values (Fig. 3a), while no further significant changes in H_p are observed. Cold plastic deformation has a significant effect on the change in H_p in the first three cycles (Fig. 3b), then this effect decreases, which indicates a significant convergence of the structural state of the steels when the number of cycles is more than three. This

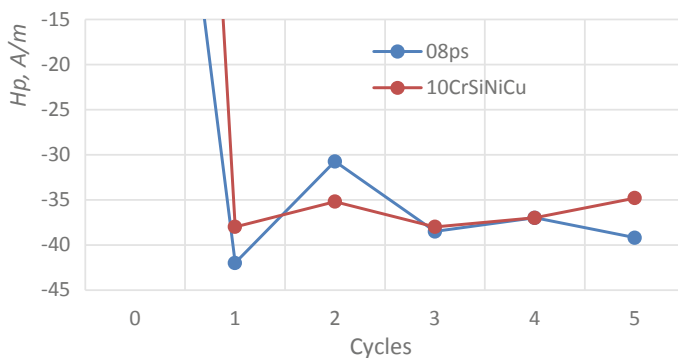


Fig. 2 Dependence of the magnetic field strength H_p on the number of cycles during thermal cycling of 08 ps and 10KhSND steels as delivered

dependence of H_p on the number of thermal cycles has a positive character, since it makes it possible to judge the completeness of the structure refinement process in hazardous zones of stress concentration in the elements of metal structures of construction machines under passive fluxgate control, where plastic deformation somehow took place during operation.

Thus, it can be seen that, regardless of the steel grade, after the fifth heating–cooling cycle, the difference between the maximum and minimum values of H_p of the steels under study (for different initial structural states) is approximately the same and amounts to 4 A/m, which indicates a relatively close final structural state of these steels after thermal cycling. An increase in the number of cycles to 10 almost does not reduce the scatter of the H_p parameter values.

The chemical composition of steels has a significant effect on the change in the stray magnetic field strength H_p . As we can see from Fig. 4, the H_p parameter undergoes the greatest changes in low-carbon steel 08 ps and the smallest in low-alloy steel 10KhSND.

The initial structure of steels also has a significant effect on the change in H_p depending on the number of thermal cycles. Thus, steels with the coarse-grained and more equilibrium structure (as delivered state + annealing at 900 °C), as compared to finer-grained steels in the as delivered state (Fig. 3a and Fig. 2, respectively), have smaller changes in H_p , starting from the 1st cycle. Steels that have undergone preliminary cold plastic deformation are characterized by more significant fluctuations in the values of H_p , especially at the 2nd and 3rd thermal cycles (Fig. 3b).

It should be noted that changes in the strength H_p depending on the chemical composition of steels, the initial microstructure, and the number of cycles are associated with structural changes in steels that occur during thermal cycling. Typical microstructures of steels after thermal cycling are shown in Figs. 5, 6, 7, 8 and 9. Metallographic studies have shown that, regardless of the initial state of the samples, a fine-grained structure is formed in all studied steels after the 3rd cycle. A further increase in the number of cycles less significantly refines the structures, which is

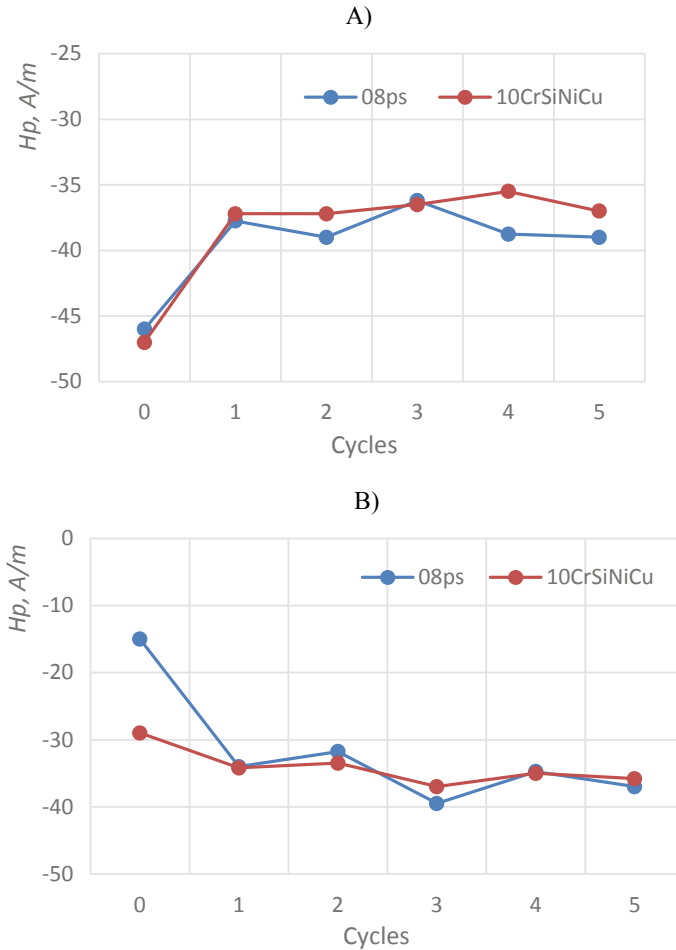


Fig. 3 Dependence of the stray magnetic field strength H_p on the number of cycles during thermal cycling of steels 08 ps and 10KhSND after preliminary annealing at 900 °C (a) and cold plastic deformation by $\varepsilon = 50\%$ (b)

consistent with the data on changes in the magnetic field strength: in subsequent cycles, a decrease in the amplitude of fluctuations in the magnetic field strength is noted.

Significant grain refinement in some areas in comparison with others after the 1st thermal cycle was also established by metallographic studies in [10]. A further increase in the number of cycles refined the structure in all areas.

It should be noted that in low-alloy steel 10KhSND, in comparison with low-carbon steel 08 ps, a finer-grained structure is formed after 5-fold thermal cycling. In addition, in alloy steel, a greater number of thermal cycles is required to obtain a fine-grained structure without noticeable grain variation than for carbon steel. Probably,

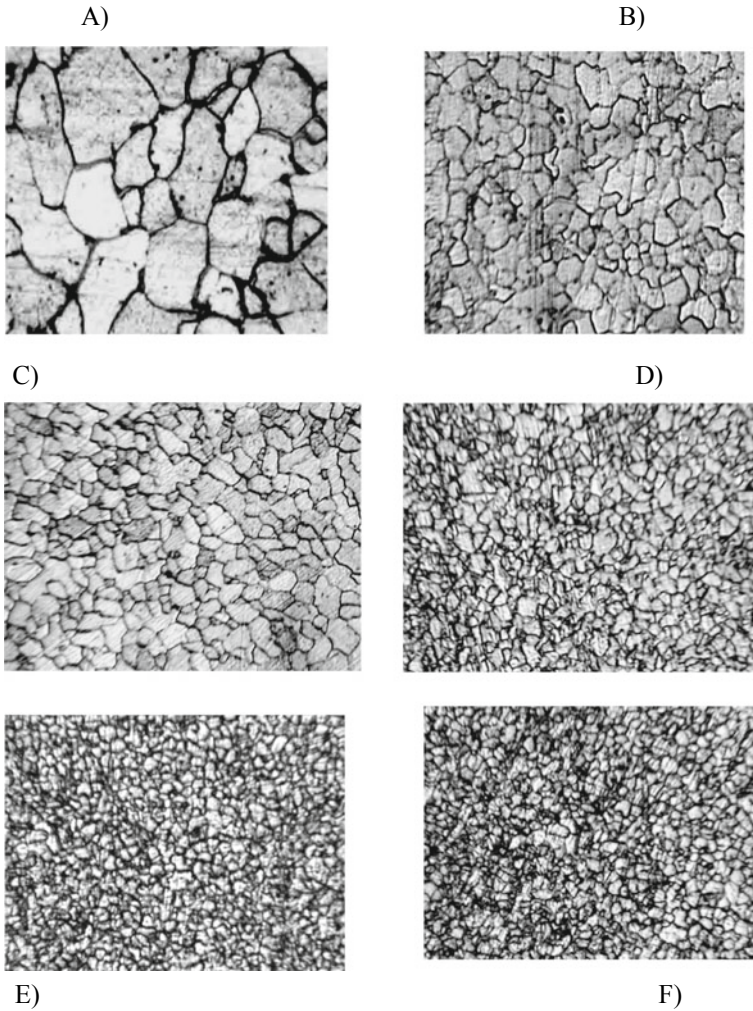


Fig. 4 Change in the structure of 08 ps steel during thermal cycling, $\times 650$: **a** as delivered, **b–f** after 1–5 cycles, respectively

the answer must be sought in the influence of alloying elements on the formation of the final structure of steel during thermal cycling.

Alloyed steels differ in that the thermodynamic activity of carbon in them is lower than in carbon steels. Therefore, a slowdown in the diffusion processes of cementite dissolution and its release from austenite leads to a shift of the C-shaped curve of isothermal decomposition of austenite to the right, making supercooled austenite more stable. Moreover, the previously described methods of thermal cycling of carbon steels can be applied to alloyed steels of the pearlite class without significant

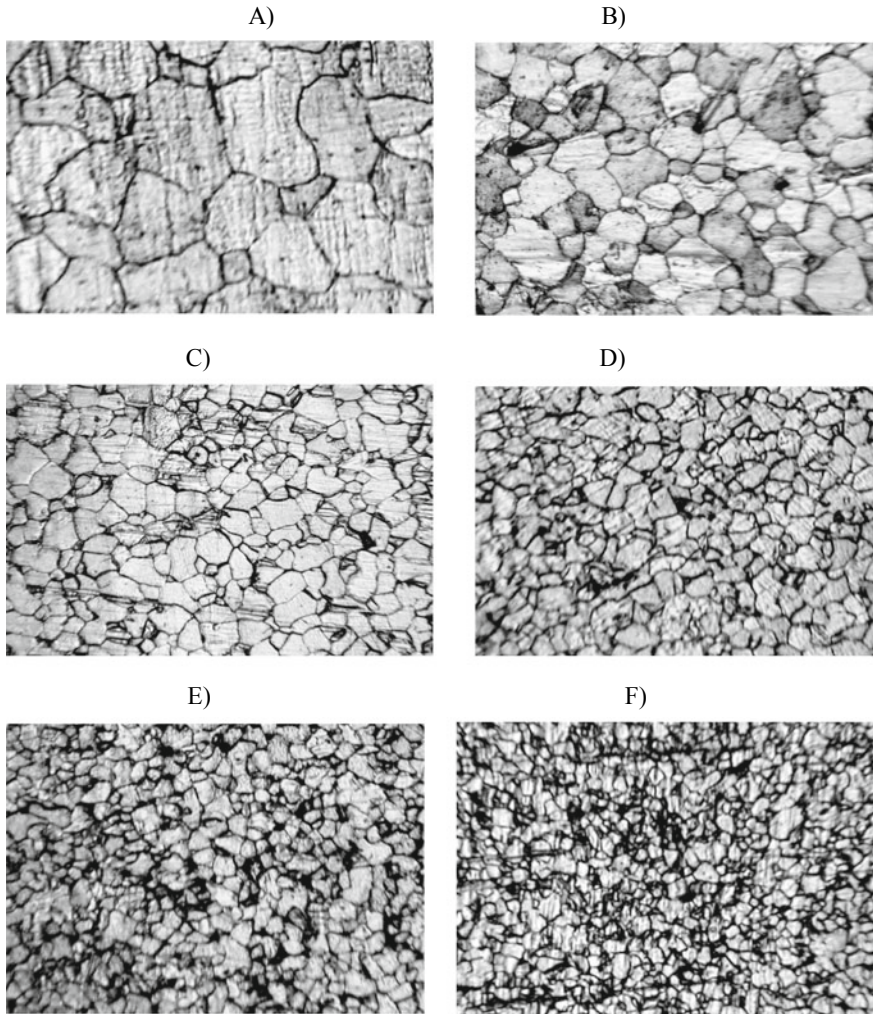


Fig. 5 Change in the structure of 08 ps steel during thermal cycling, $\times 650$: **a** state (as delivered + annealing at 900 °C), **b–f** after 1–5 cycles, respectively

changes in technology, when the total content of alloying elements does not exceed 5%.

During thermal cycling, phase and structural transformations in steels are accompanied by the formation, displacement and annihilation of point and linear defects, as well as the redistribution of alloying elements. In the process of thermal cycling, the existing dislocations are set in motion, while the formation and multiplication of new dislocations takes place. During thermal cycling of iron, an increase in the dislocation density begins immediately after the start of treatment. With an increase in the number of cycles (thermal cycling time), the dislocation density increases.

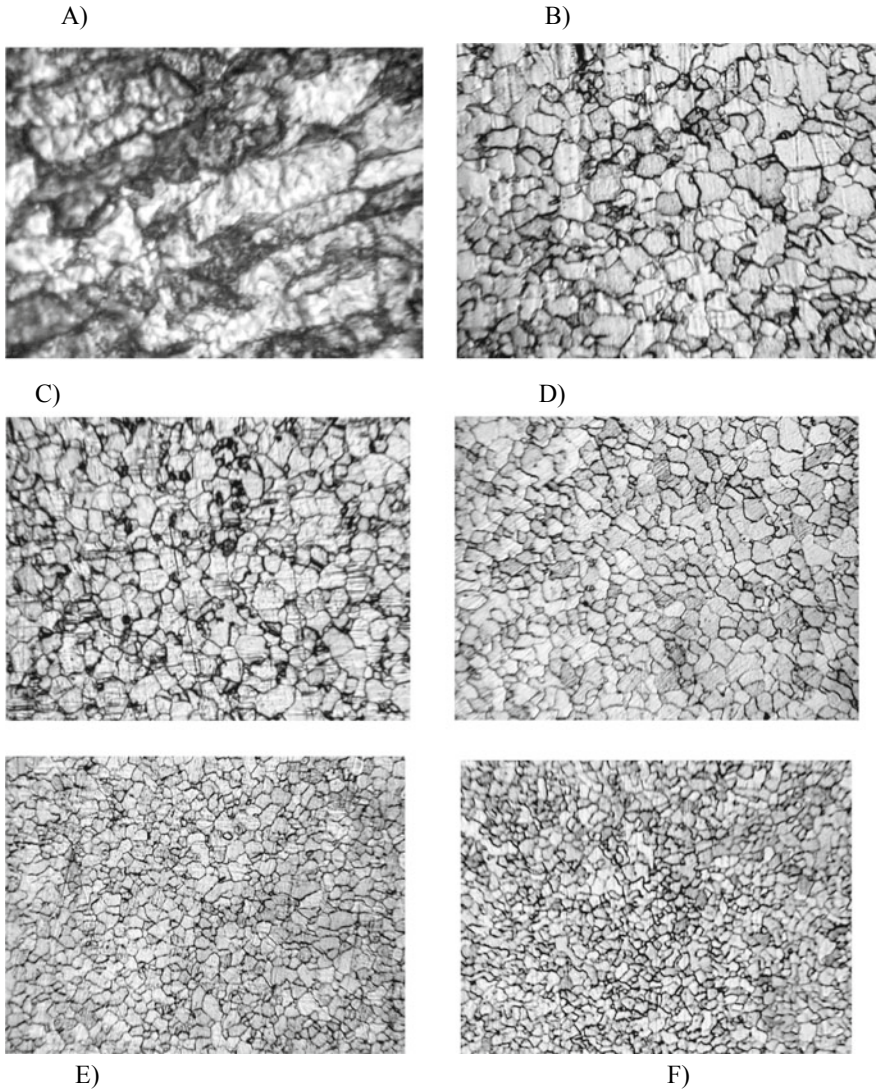


Fig. 6 Change in the structure of steel 08 ps during thermal cycling, $\times 650$: **a** condition (as delivered + rolling by $\varepsilon = 50\%$), **b-f** after 1–5 cycles, respectively

Consequently, the efficiency of thermal cycling will be determined by the degree of generation of defects and, first of all, dislocations.

During thermal cycling, there is a sharp change in the microstructure, substructure, and dislocation structure. The main structural change in steel is significant grain refinement, be it pearlite, ferrite, martensite, or other structure. Moreover, the

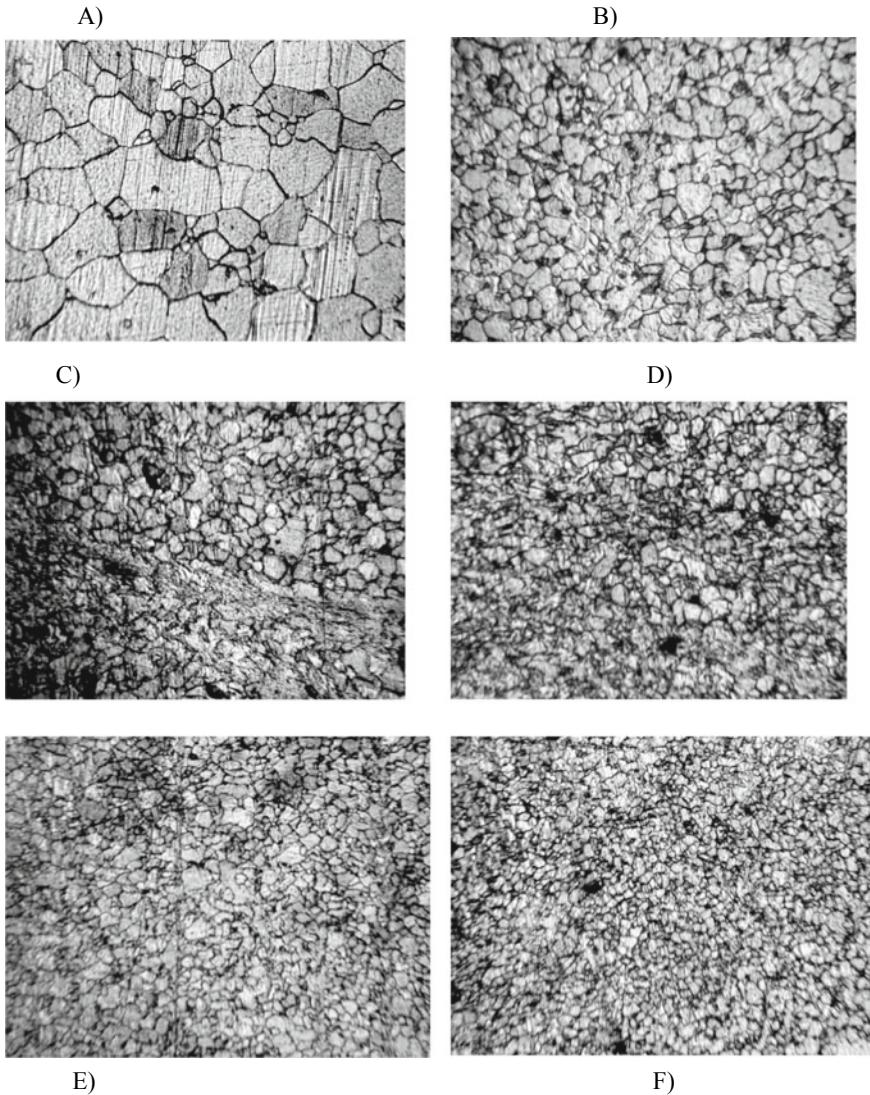


Fig. 7 Change in the structure of steel 10KhSND during thermal cycling, $\times 650$: **a** as delivered, **b–f** after 1–5 cycles, respectively

grinding of grains, as a rule, is accompanied by a decrease in grain size and a more uniform distribution of chemical elements.

The main reason for such changes in the structure is the intensification of diffusion processes due to the intensification of the effect of thermophysical factors. In the process of thermal cycling, the existing dislocations are set in motion, while the formation and multiplication of new dislocations takes place. During thermal cycling

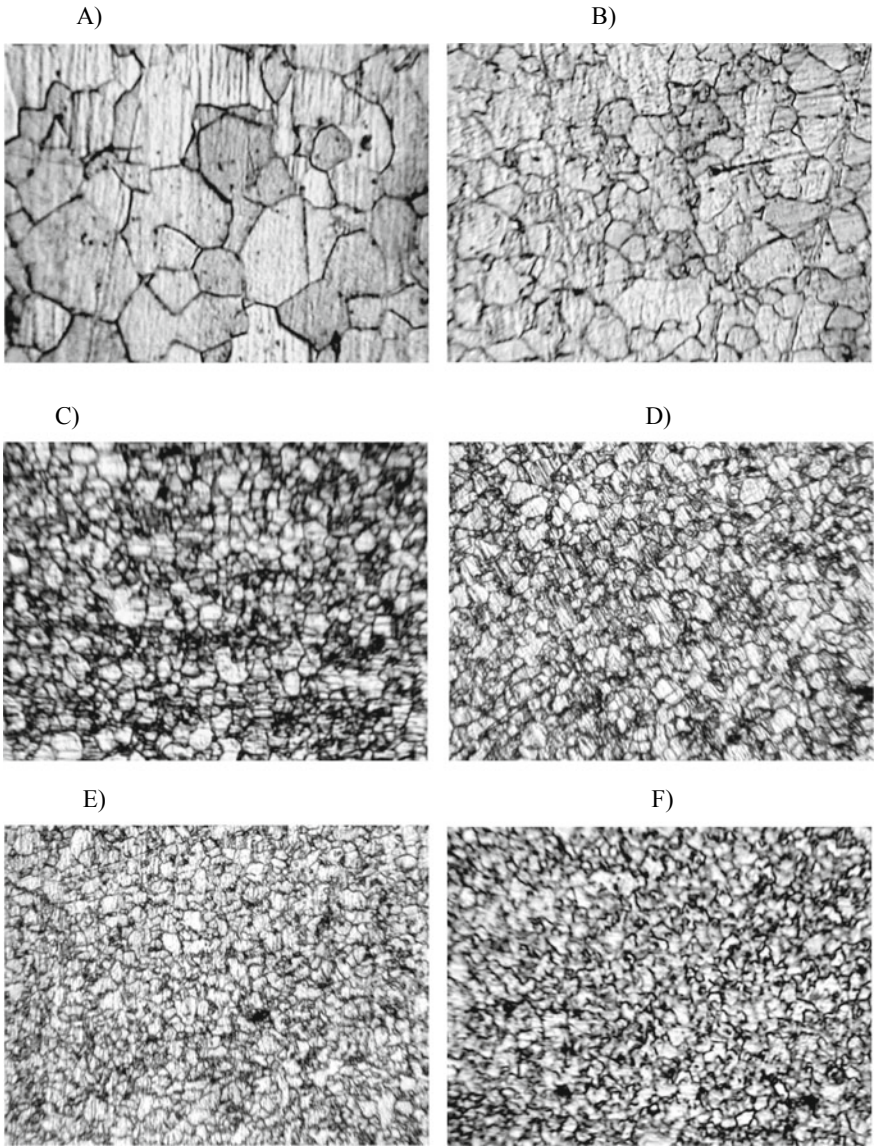


Fig. 8 Change in the structure of steel 10KhSND during thermal cycling, $\times 650$: **a** state (as delivered + annealing at 900 °C), **b–f** after 1–5 cycles, respectively

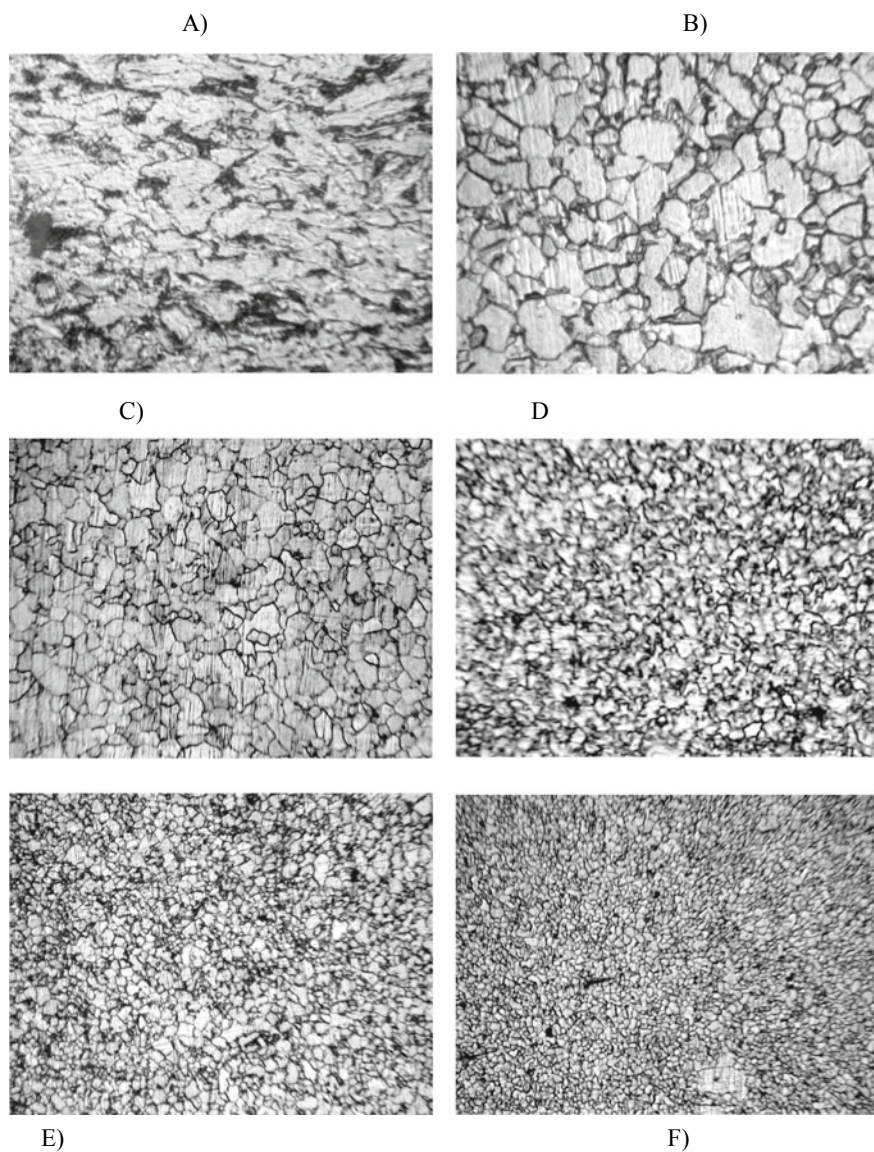


Fig. 9 Change in the structure of steel 10KhSND during thermal cycling, $\times 650$: **a** condition (as delivered + rolling by $\varepsilon = 50\%$), **b-f** after 1-5 cycles, respectively

of iron, zirconium, tungsten, as well as low-temperature thermal cycling of molybdenum, an increase in the dislocation density begins immediately after the start of treatment.

The accumulation of dislocations and the formation of a polygonal substructure after thermal cycling of pure iron and low-carbon steel suggest that polymorphic transformations are responsible for the formation of a dislocation structure during thermal cycling of steels, leading to phase hardening mainly due to the difference in specific volumes and elastic moduli of the formed phases. Phase hardening is sometimes accompanied by recrystallization processes, which, with the accumulation of deformation, are monotonously repeated from cycle to cycle.

Recrystallization centers are formed, first of all, in those areas of the lattice that are most distorted, including at the grain boundaries and their joints, which leads to the formation of a fine-grained structure. The recrystallization process during thermal cycling can be represented as a multiple alternation of small deformations and recrystallization annealing.

In the light of the above, it becomes clear why in low-alloy steel 10KhSND, in comparison with low-carbon steel 08 ps, the process of decreasing grain size is shifted towards a larger number of cycles. This is explained by the fact that in alloyed steels, the thermodynamic activity of carbon is lower than in carbon steels, and, consequently, structural changes during thermal cycling in them occur more slowly. Therefore, the influence of alloying elements on the number of cycles during thermal cycling is such that with an increase in their percentage in steel, an increase in the number of cycles is required to obtain an equiaxed fine-grained structure.

The microstructure of steels before thermal cycling significantly affects the final grain size. The coarser-grained initial structure of steels (as delivered + annealing at 900 °C), in comparison with the as delivered structure, also corresponds to the coarser-grained structure after thermal cycling (Figs. 4, 5, 7 and 8). Figure 5 shows the structure of steel 08 ps after five-time thermal cycling. Before thermal cycling, the as delivered samples were annealed for 30 min at 900 °C, as a result of which an equilibrium structure was formed in them. In this case, as in the thermal cycling of as delivered samples, after the first cycle, a structure with different grain sizes is formed in different areas. However, the graininess in this case is somewhat less, and the grain size is larger. In subsequent cycles, further refinement of the grains occurs, and after the fifth cycle, a fairly homogeneous structure with fine grains is formed. The structure of steel 10KhSND at different stages of processing, in comparison with the previous steels, has a lower grain size difference, and after the fifth cycle, it has a homogeneous fine-grained structure. It should be noted that with an increase in the degree of alloying of steels, a finer-grained structure is formed in them, both in the state (as delivered + annealing at 900 °C) and in the as delivered state.

Consequently, during thermal cycling, when grain growth is suppressed by low austenitization temperatures and short holding times, the optimal initial structure will be such a structure that provides the maximum density of carbides at high-angle boundaries of ferrite grains. In our case, steel 10KhSND may have such an opportunity.

The presence of a deformed structure before thermal cycling makes significant adjustments for both carbon steel 08 ps and low-alloy steel 10KhSND (Figs. 7 and 8). A significant difference between the thermal cycling of pre-deformed samples is the obtaining of a finer-grained structure than that of the as delivered samples and in the state (as delivered + annealing at 900 °C), which is associated with the activation of structural changes that occur during heating and cooling.

A significant refinement of the structure during thermal cycling after cold plastic deformation is explained by the fact that cold deformation redistributes and increases the density of imperfections in the crystal structure of dislocations, vacancies, stacking faults, and, in addition, promotes the formation and development of low and high angle boundaries. Since crystal lattice defects strongly affect the formation of the structure of alloys during phase and structural transitions, plastic deformation in front of them, as well as during their passage, can be effectively used to create an optimal structure during thermal cycling of steels.

A more intense passage of structural changes during thermal cycling of cold-worked steels and the final formation of an equiaxed fine-grained structure after the third cycle is confirmed by a change in the H_p values during cyclic annealing. So, from Fig. 3c, it can be seen that the values of H_p for the studied steels after the 4th and 5th cycles are almost equal, which indicates the end of the effective refinement of the grain size and the formation of a fine-grained structure. Consequently, using the magnetic method, it becomes possible to control the formation of the finest-grained structure in low-carbon and low-alloy steels at the early stages of their thermal cycling.

4 Conclusions

As a result of the conducted studies, a relationship was established between the magnetic parameter H_p and structural changes in steels during thermal cycling. It is shown that the magnitude of the stray magnetic field strength H_p depends on the initial microstructure, the chemical composition of the steels, and the number of thermal cycles.

The greatest change in the values of the stray magnetic field strength H_p is observed during the first heating–cooling cycles. Their further increase decreases the magnetic amplitude, which is associated with a less significant refinement of the structure during subsequent cycles. This type of change in H_p values can be used to control the formation of a fine-grained structure in low-carbon and low-alloy steels during thermal cycling.

References

1. Scherbakov AP (2020) Experimental studies of heat treatment influence on the welded connections properties in working mechanisms of road building. *Russ Automob Highway Ind J* 17(6):664–675
2. Scherbakov A, Monastyreva D, Smirnov V (2019) Passive fluxgate control of structural transformations in structural steels during thermal cycling. *E3S Web of Conferences*, vol 135, 03022. <https://doi.org/10.1051/e3sconf/201913503022>
3. Scherbakov A, Babanina A, Graboviy K (2021) Acting stresses in structural steels during elastoplastic deformation. *Adv Intell Syst Comput* 1259:298–311
4. Lupachev AV, Pavlyuk SK (2019) Determination of electrode potentials on local surfaces of metals and welded joints. *Factory laboratory. Diagnost Mater* 8:43–46
5. Scherbakov AP, Pushkarev AE, Vinogradova TV (2021) Influtnce analysis of 09Г2С and 30MnB5 steels thermocyclic treatment on strength characteristics of road construction machines working bodies. *Russ Automobile Highw Ind J* 18(2):180–190. (In Russ.) <https://doi.org/10.26518/2071-7296-2021-18-2-180-190>
6. Scherbakov A, Babanina A, Kochetkov I, Khoroshilov P (2020) Technical condition of welded load-bearing metal structures of operated agricultural hoisting cranes. *E3S Web of Conferences*, vol 175, 11005. <https://doi.org/10.1051/e3sconf/202017511005>
7. Scherbakov AP (2020) Material and method selection for increasing the wear resistance of construction machines components. *Russ Automob Highway Ind J* 17(4):464–475
8. Fireushin AM, Fatkullin MR, Ulyabaev RR, Chernyatyevev RR, Kadoshnikova AV (2018) Improving the technology for repairing cases of thick-walled machines and assemblies. *Neftegazovoe delo* 16(3):76–83
9. Plotnikov DG (2015) Methods for assessing the strength of metal structures of hoisting-and-transport machines. *Nauchno-tekhnicheskie vedomosti SPbGPU* 1(214):186–193
10. Scherbakov A, Babanina A, Matusevich A (2021) Passive probe-coil magnetic field test of stress-strain state for welded joints. *Adv Intell Syst Comput* 1259:312–323